J Mater Sci (2008) 43:2857–2864
DOI 10.1007/s10853-007-2263-9

Microstructure, electrical properties, and dc aging characteristics of Tb_4O_7-doped ZnO-based varistors

Choon-Woo Nahm

Received: 28 April 2007 / Accepted: 26 October 2007 / Published online: 9 February 2008

Abstract The microstructure, electrical properties, and dc-accelerated aging characteristics of Tb_4O_7-doped ZnO-based varistors were investigated for different Tb_4O_7 amounts and sintering temperatures. The sintered density increased with increasing Tb_4O_7 amount and sintering temperature. The average grain size decreased with increasing Tb_4O_7 amount and increased with increasing sintering temperature. The varistor voltage and nonlinear coefficient increased with increasing Tb_4O_7 amount and decreased with increasing sintering temperature. The stability was worse with increasing Tb_4O_7 amount for the varistors sintered at 1,300 °C. The 0.5 mol% Tb_4O_7-doped varistors sintered at 1,350 °C exhibited a good stability for dc-accelerated aging stress of 0.95 $V_{1\ mA}$/150 °C/24 h.

Introduction

The increasing use of semiconductors and other solid-state components in modern electrical systems has resulted in a growing awareness about system reliability. This is a consequence of the fact that solid-state devices are very susceptible to stray electrical transient, which may appear in the low-voltage ac distribution system. The initial use of semiconductors resulted in a large number of unexplainable failures. Investigation into these failures revealed that they were caused by a number of diverse overvoltage conditions, which were present in the distribution system. Transient voltages result from the sudden release of previously stored energy from overstress conditions such as lightning, inductive load switching, electromagnetic pulses, or electrostatic discharges. Therefore, electrical and electronic systems should be protected from various surges. One way to overcome these surges is to enhance the insulating strength for devices and systems. Another way is to use varistors. Zinc oxide (ZnO) varistors are smart two-terminal semiconductor-ceramic devices made by sintering ZnO powder with small amounts of minor additives, containing varistor-forming oxides (VFO) such as Bi_2O_3, Pr_6O_{11}, V_2O_5, BaO, La_2O_3, and so on [1, 2]. They exhibit highly nonlinear voltage–current (V–I) characteristics: electrical impedance of a varistor decreases abruptly at increased voltage, and at a certain point, they behave as a short circuit. They possess excellent surge-energy-absorption capabilities. As a result, they have been extensively used to protect various semiconductor devices, electronic equipment, and electric power systems from dangerous abnormally high voltage [1, 2]. The nonlinear properties of ZnO varistors are attributed to a double Schottky barrier (DSB) formed at active grain boundaries containing many trap states.

Most commercial ZnO varistors contain Bi_2O_3 as a VFO and they exhibit excellent varistor properties and high performance. However, they have a few drawbacks due to the high volatility and reactivity of Bi_2O_3, which melts at about 825 °C during sintering above 1,000 °C [3]. The former changes varistor characteristics with the variation of intercomposition ratio of additives, the latter destroys the multilayer structure of chip varistors, and it generates an insulating spinel phase deteriorating surge-absorption capabilities.

Recently, ZnO–Pr_6O_{11}-based nonlinear resistors have been studied in order to improve a few drawbacks [3] associated with Bi_2O_3 [4–11]. Nahm et al. reported that Zn–Pr–Co–Cr–REO (REO = Er, Y, Dy, La)-based nonlinear resistors have highly nonlinear properties [6–11]. To

C.-W. Nahm (✉)
Department of Electrical Engineering, Dongeui University, Busan 614-714, Korea
e-mail: cwnahm@deu.ac.kr

develop nonlinear resistors of high performance, it is very important to comprehend the effects of the additives on nonlinear properties.

In the present study, the effect of Tb_4O_7 addition and sintering temperature on the microstructure, electric field–current density (E–J) characteristics, capacitance–voltage (C–V) characteristics, and dc aging characteristics of Zn–Pr–Co–Cr–Tb oxide-based varistors was examined. In particular, it was found that the stability was greatly affected by the Tb_4O_7 amount and sintering temperature.

Experimental procedure

Sample preparation

Reagent-grade raw materials were used in proportions of (98.0-x) mol% ZnO, 0.5 mol% Pr_6O_{11} ,1.0 mol% CoO, 0.5 mol% Cr_2O_3, x mol% Tb_4O_7 ($x = 0.25$, 0.5, 1.0). Raw materials were mixed by ball milling with zirconia balls and acetone in a polypropylene bottle for 24 h. The mixture was dried at 120 °C for 12 h and calcined in air at 750 °C for 2 h. The calcined mixture was pulverized using an agate mortar/pestle, and after 2 wt.% polyvinyl alcohol (PVA) binder addition, granulated by sieving through a 100-mesh screen to produce the starting power. The power was pressed into 10 mm diameter and 2 mm thickness at a pressure of 80 MPa. The disks were sintered at two fixed sintering temperatures of 1,300 and 1350 °C in air for 1 h and furnace-cooled to room temperature. The heating and cooling rates were 4 °C/min. The sintered samples were lapped and polished to 1.0 mm thickness. The final samples were about 8 mm in diameter and 1.0 mm in thickness. Silver paste was coated on both faces of samples and the electrodes were formed by heating at 600 °C for 10 min. The electrodes were 5 mm in diameter.

Microstructure measurement

Both surfaces of the samples were lapped and ground with SiC paper and polished with 0.3 μm-Al_2O_3 powder to a mirror-like surface. The polished samples were thermally etched at 1,100 °C for 30 min. The surface of samples was metallized with a thin coating of Au to reduce charging effects and to improve the resolution of the image. The surface microstructure was examined by a scanning electron microscope (SEM, Hitachi S2400, Japan). The average grain size (d) was determined by the lineal intercept method by the following expression [12]:

$$d = 1.56L/MN \tag{1}$$

where L is the random line length on the micrograph, M is the magnification of the micrograph, and N is the number of the grain boundaries intercepted by lines. The compositional analysis of the selected areas was determined by an attached energy dispersion X-ray analysis (EDX) system. The crystalline phases were identified by an X-ray diffractometry (XRD, Rigaku D/max 2100, Japan) using a CuK_α radiation. The sintered density (ρ) of varistor ceramics was measured by the Archimedes method.

Electrical measurement

The voltage–current (V–I) characteristics of the varistors were measured by stepping up the linear stair voltage using a high-voltage source-measure unit (Keithley 237). The varistor voltage ($V_{1\ \mathrm{mA}}$) was measured at 1.0 mA/cm^2 and the leakage current (I_L) was measured at 0.80 $V_{1\ \mathrm{mA}}$. In addition, the nonlinear coefficient (α) was calculated by the following equation:

$$\alpha = 1/(\log E_2 - \log E_1) \tag{2}$$

where E_1 and E_2 are the electric fields corresponding to 1.0 and 10 mA/cm^2, respectively.

The capacitance–voltage (C–V) characteristics of varistors were measured at 1 kHz with the variable applied bias in the pre-breakdown region of the V–I characteristics using a QuadTech 7600 RLC meter and a Keithley 617 electrometer. The donor density (N_d) of ZnO grains and the barrier height (Φ_b) at the grain boundary were determined from the slope and intercept of straight line, respectively, using the following equation [13]:

$$(1/C_b - 1/2C_{bo})^2 = 2(\Phi_b + V_{gb})/q\varepsilon N_d \tag{3}$$

where C_b is the capacitance per unit area of a grain boundary, C_{bo} is the value of C_b when $V_{gb} = 0$, V_{gb} is the applied voltage per grain boundary, q is the electronic charge, ε is the permittivity of ZnO ($\varepsilon = 8.5\varepsilon_o$). The density of interface states (N_t) at the grain boundary was determined by the following equation [13]:

$$N_t = (2\varepsilon N_d \Phi_b / q)^{1/2} \tag{4}$$

Once the donor density and barrier height were known, the depletion layer width (t) of the either side at the grain boundaries was determined by the following equation [14]:

$$N_d t = N \tag{5}$$

dc-accelerated aging characteristic measurement

The dc-accelerated aging stress test was performed under four continuous conditions:

(i) the 1st stress: 0.85 $V_{1\ mA}$/115 °C /24 h
(ii) the 2nd stress: 0.90 $V_{1\ mA}$/120 °C /24 h
(iii) the 3rd stress 0.95 $V_{1\ mA}$/125 °C /24 h
(iv) the 4th stress: 0.95 $V_{1\ mA}$/150 °C /24 h.

Simultaneously, the leakage current was monitored at intervals of 1 min during stressing using a high-voltage source-measure unit (Keithley 237). The degradation rate coefficient (K_T) was calculated from the following equation [15]:

$$I_L = I_{Lo} + K_T t^{1/2} \quad (6)$$

where I_L is the leakage current at stress time (t) and I_{Lo} is I_L at $t = 0$. After the respective stresses, the V–I characteristics were measured at room temperature. In processing numerical data, 5 samples for varistors (sintered for the same time) were used for all electrical measurements and their average value is presented.

Results and discussion

Figure 1 shows SEM micrographs of the varistor ceramics with different Tb_4O_7 amounts and sintering temperatures. The microstructure of ZnO–Pr_6O_{11}-based varistor ceramics consisted of only two phases, mainly ZnO grain (blackish) and intergranular layer (whitish) as a secondary phase. The SEM micrographs remarkably show two phases, i.e., ZnO grains and intergranular layers regardless of Tb_4O_7 amounts and sintering temperature. An intergranular layer consisted of Tb- and Pr-rich phases by XRD analysis, as indicated in Fig. 2. It was found from EDX of Fig. 3 that they coexist at the grain boundaries and the nodal points as if they were a single phase. It was observed by SEM that as the Tb_4O_7 amount increased, the intergranular phase gradually became more distributed at the grain boundaries and particularly at the nodal points. The detailed microstructural parameters are summarized in Table 1.

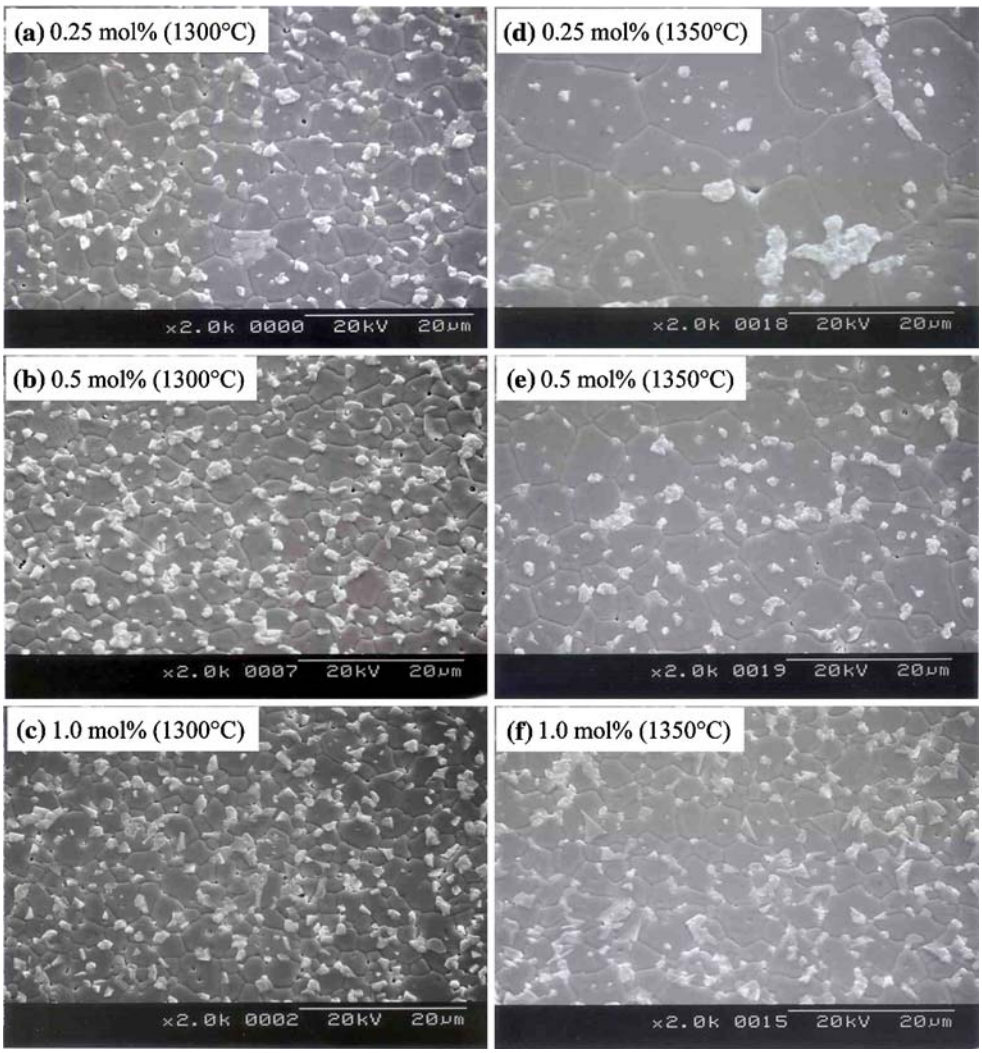

Fig. 1 Micrographs of the varistor ceramics doped with different Tb_4O_7 amounts at different sintering temperatures

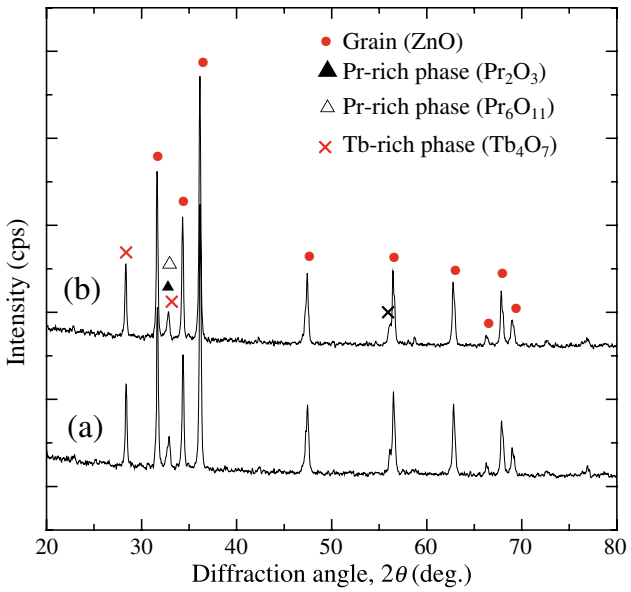

Fig. 2 XRD analysis of 1.0 mol% Tb_4O_7-doped varistor ceramics at different sintering temperatures: (**a**) 1,300 °C, (**b**) 1,350 °C

With increasing Tb_4O_7 amount, the average grain size of the sintered ceramics decreased in the range of 5.1–4.2 μm at 1,300 °C and 10.1–5.0 μm at 1,350 °C. Therefore, Tb_4O_7 was found to serve as an inhibitor of grain growth. It was found that the sintered density of ceramics sintered is in the range of 5.74–5.83 g/cm^3 corresponding to 99.3–100.9% of theoretical density (TD = 5.78 g/cm^3 in ZnO) at 1,300 °C and 5.75–5.85 g/cm^3 corresponding to 99.5–101.2% of TD at 1,350 °C. The ceramics were more densified with increasing Tb_4O_7 amount. On the whole, the ceramics sintered at 1,350 °C were slightly more densified than those sintered at 1,300 °C.

Figure 4 shows the electric field–current density (E–J) characteristic curves of varistors with different Tb_4O_7 amounts and sintering temperatures. For both sintering temperatures, the current density increased linearly in low field, whereas it varied by orders of magnitude with only small changes in field above the breakdown field, so called a varistor voltage. On adding more Tb_4O_7, the knee gradually becomes more pronounced and the nonlinear properties are enhanced. Therefore, the addition of Tb_4O_7 seems to remarkably enhance nonlinear properties. The variations of V–I characteristic parameters, including the varistor voltage ($V_{1\ mA}$), varistor voltage per grain boundary (V_{gb}), nonlinear coefficient (α), and leakage current (I_L), are summarized in Table 1. As the Tb_4O_7 amount increased, the $V_{1\ mA}$ was found to increase in the range of 538.0–845.1 V/mm for varistors sintered at 1,300 °C and 140.8–651.4 V/mm at 1,350 °C. It can be seen that the Tb_4O_7-doped varistors provide very high-voltage varistors. Therefore, it can be applied to the compact size. The $V_{1\ mA}$ is directly related to the number of grain boundaries across

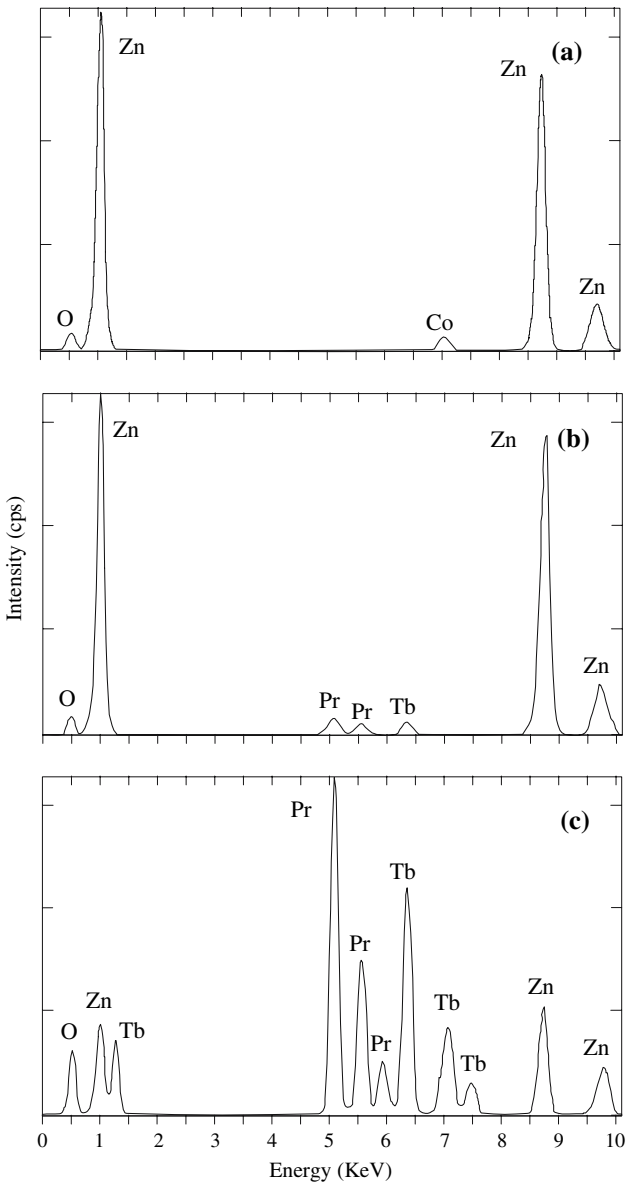

Fig. 3 EDX analysis of the varistor ceramics doped with Tb_4O_7: (**a**) ZnO grain, (**b**) Grain boundary, (**c**) Intergranular layer

a series between the electrodes. Therefore, the increase of $V_{1\ mA}$ with increasing Tb_4O_7 amount is attributed to the decrease of average grain size caused by Tb_4O_7 addition which inhibits grain growth, as mentioned when discussing microstructure previously. The decrease of $V_{1\ mA}$ at higher sintering temperature can be explained by the same reasoning. The V_{gb} that is a varistor voltage per grain boundary is defined by the following equation:

$$V_{gb} = (d/D) \cdot V_{1\,mA} \tag{7}$$

where d is the average grain size and D is the thickness of the sample. The V_{gb} was in the range of 2.8–3.6 V/gb for the varistors sintered at 1,300 °C and 1.4–3.3 V/gb at 1,350 °C with Tb_4O_7 amount. This was within the general

Table 1 Microstructure, *V–I*, and *C–V* characteristic parameters of the varistors doped with different Tb_4O_7 amounts at diffferent sintering temperatures

Sintering temp. (°C)	Tb_4O_7 amount (mol%)	d (μm)	ρ (g/cm^3)	$V_{1\ mA}$ (V/mm)	V_{gb} (V/gb)	α	I_L (μA)	N_d (10^{18}/cm^3)	N_t (10^{12}/cm^2)	Φ_b (eV)	t (nm)
1,300	0.25	5.1	5.74	538.0	2.8	33.9	1.5	0.83	2.84	1.04	34.2
	0.5	4.3	5.77	705.2	3.0	42.4	1.2	0.82	2.81	1.03	34.3
	1.0	4.2	5.83	845.1	3.6	52.0	5.9	0.78	2.70	0.99	34.6
1,350	0.25	10.1	5.75	140.8	1.4	18.6	4.6	1.05	2.68	0.73	21.8
	0.5	7.3	5.80	299.1	2.2	31.7	1.7	0.99	2.67	0.77	21.7
	1.0	5.0	5.85	651.4	3.3	42.0	3.0	0.70	2.48	0.93	35.4

value of 2–3 V/gb regardless of sintering processes. However, generally, the higher the value, the higher the nonlinear properties.

One of the most important figures of merit in varistors is the nonlinear coefficient, α, which characterizes the native properties of the varistor itself. The α value linearly increased in the range of 33.9–52.0 for the varistors sintered at 1,300 °C. On the other hand, the α value linearly increased in the range of 18.6–42.0 for the varistors sintered at 1,350 °C. The increase of sintering temperature in equivalent compositions led to low nonlinearity. It is postulated that the rare earth oxide (REO), Tb_4O_7, is involved in the formation of interfacial states and deep bulk traps, both of which contribute to the highly nonlinear properties. It can be seen that the increase of Tb_4O_7 amount improves nonlinear properties. The I_L values varied with ^-shaped in the range of 1.2–5.9 μA for the varistors sintered at 1300°C and in the range of 1.7–4.6 μA at

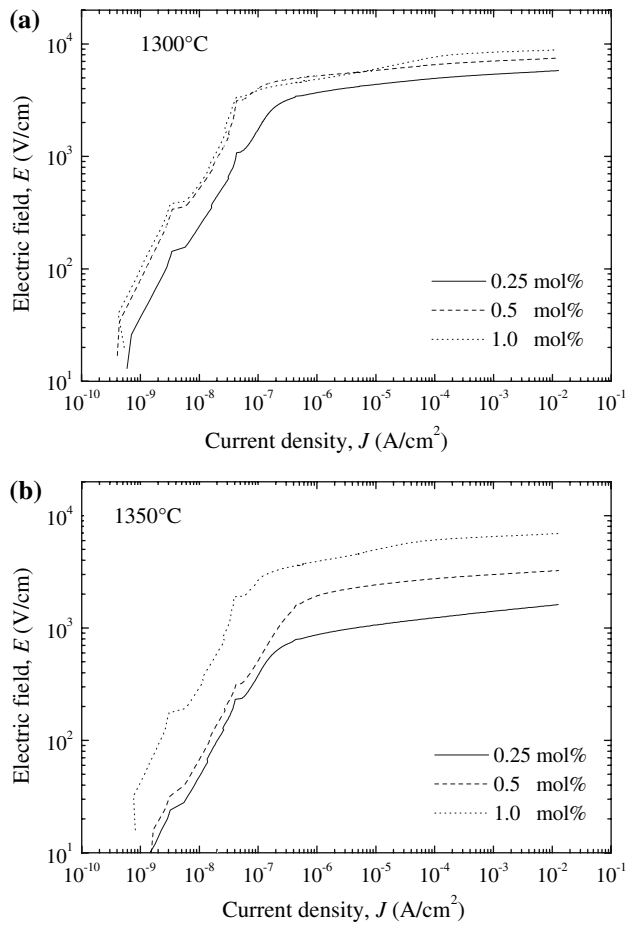

Fig. 4 *E–J* characteristics of the varistors doped with different Tb_4O_7 amounts at different sintering temperatures

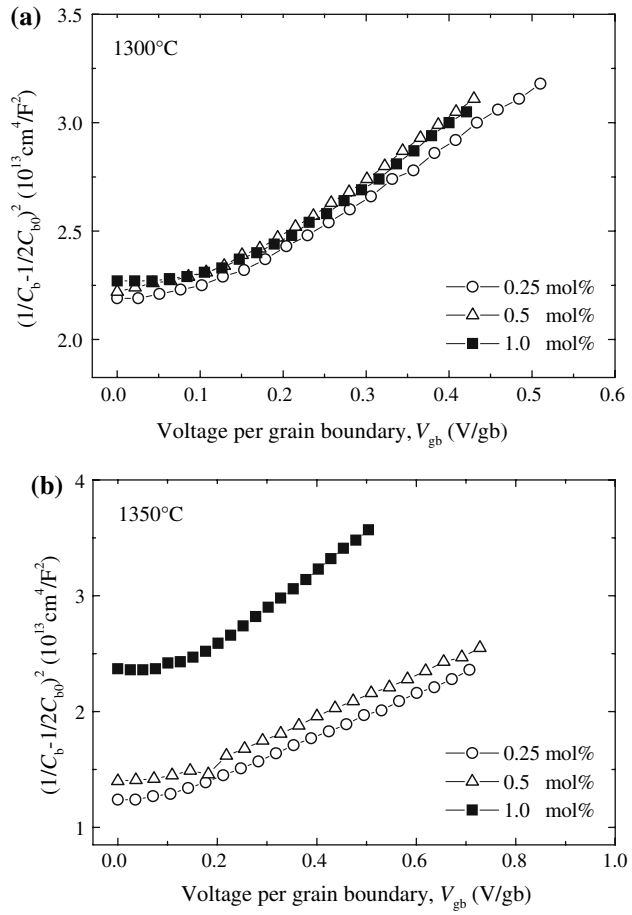

Fig. 5 *C–V* characteristics of the varistors doped with different Tb_4O_7 amounts at different sintering temperatures

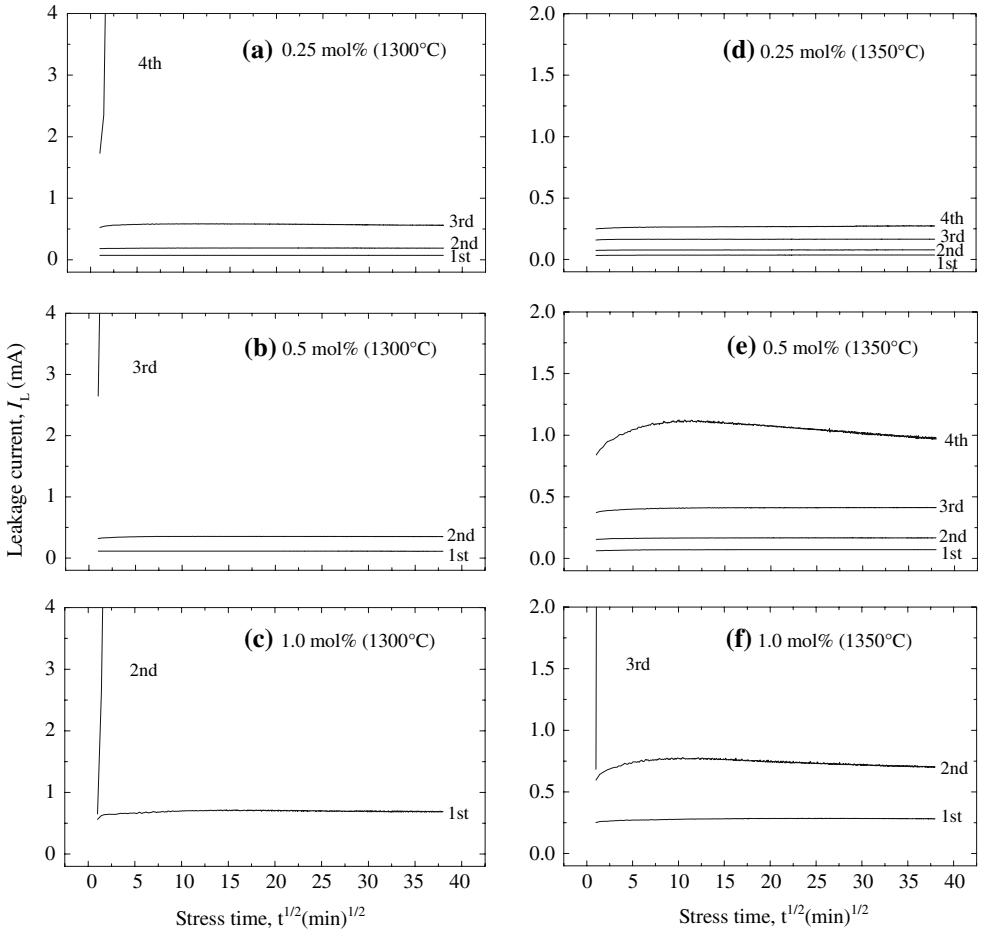

Fig. 6 Leakage current during dc-accelerated aging stress of the varistors doped with different Tb_4O_7 amounts at different sintering temperatures

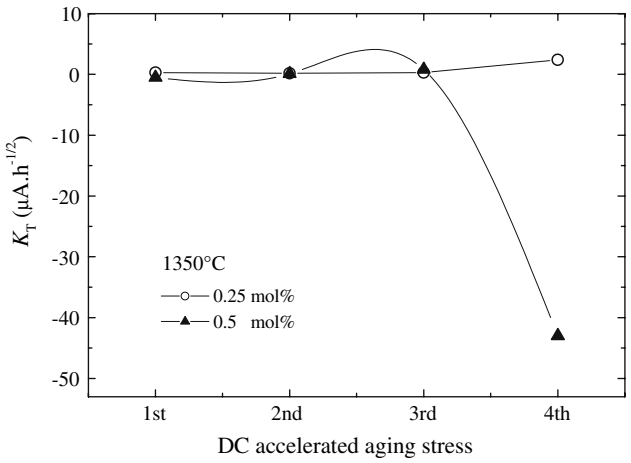

Fig. 7 Degradation rate coefficient of the 0.25 and 0.5 mol% Tb_4O_7-doped varistors sintered at 1,350 °C

1,350 °C, with a minimum value at 0.5 mol% Tb_4O_7 for both sintering temperatures. As a result, it is assumed that the Tb_4O_7 significantly affects *V–I* characteristics.

Figure 5 shows the *C–V* characteristics of varistors with different Tb_4O_7 amounts and sintering temperatures. It is assumed that the *C–V* characteristics for sintering temperature will be various because the *C–V* characteristic curves are arranged variously according to different Tb_4O_7 amounts and sintering temperatures. The *C–V* characteristic parameters, including the donor density (N_d), density of interface states (N_t), barrier height (Φ_b), and depletion layer width (t), are summarized in Table 1. As the Tb_4O_7 amount increased, the N_d value decreased in the range of 0.83×10^{18}–0.78×10^{18}/cm^3 for varistors sintered at 1,300 °C and in the range of 1.05×10^{18}–0.70×10^{18}/cm^3 at 1,350 °C. It is assumed that the decrease of N_d is attributed to the increase of oxygen. The N_d is related to the partial pressure of oxygen (Po_2), namely, $N_d \propto Po_2^{-1/4}$ or $Po_2^{-1/6}$. The t value on either side of depletion region increased with increasing Tb_4O_7 amounts. This shows an opposite relation to the N_d. In general, the depletion region extends farther into the side with a lighter doping. The N_t value weakly decreased in the range of 2.84×10^{12}–2.70×10^{12}/cm^2 for the varistors sintered at 1,300 °C and 2.68×10^{12}–2.48×10^{12}/cm^2 at 1,350 °C with increasing Tb_4O_7 amounts. On the whole, the N_t value of varistors sintered at 1,350 °C exhibited to be lower compared with those at 1,300 °C. The Φ_b value decreased in the range of 1.04–0.99 eV for the varistors sintered at 1,300 °C and increased in the range of 0.73–

Table 2 *E–J* characteristic parameters after dc-accelerated aging stress of the varistors doped with different Tb_4O_7 amounts at different sintering temperatures

Sintering temp. (°C)	Tb_4O_7 amount (mol%)	Stress state	K_T ($\mu A \cdot h^{-1/2}$)	$V_{1\ mA}$ (V/mm)	$\%\Delta V_{1\ mA}$	α	%Δα	I_L (μA)	$\%\Delta I_L$
1,300	0.25	Before	–	538.1	0	33.9	0	1.5	0
		1st	0	537.7	−0.1	33.5	−1.2	2.3	53.3
		2nd	−0.1	537.5	−0.1	33.4	−1.5	3.3	120.0
		3rd	−5.7	537.1	0.2	33.3	−1.8	4.9	226.7
		4th	Thermal runaway						
	0.5	Before	–	705.2	0	42.4	0	1.2	0
		1st	−0.6	704.9	0	41.9	−1.2	1.7	41.7
		2nd	−0.4	704.4	−0.1	41.8	−1.4	2.6	116.7
		3rd	Thermal runaway						
	1.0	Before	–	845.1	0	52.0	0	5.9	0
		1st	−1.5	844.8	0	51.4	−1.2	5.9	0
		2nd	Thermal runaway						
1,350	0.25	Before	–	140.8	0	18.6	0	4.6	0
		1st	0.3	139.9	−0.6	18.3	−1.6	5.6	21.7
		2nd	0.2	139.6	−0.9	18.3	−1.6	5.8	26.1
		3rd	0.3	139.3	−1.1	18.2	−2.2	5.9	28.3
		4th	2.4	138.7	−1.5	18.2	−2.2	5.7	23.9
	0.5	Before	–	299.1	0	31.7	0	1.7	0
		1st	−0.5	299.2	0	31.6	−0.3	1.9	11.8
		2nd	0.1	299.4	0.1	31.9	0.6	2.1	23.5
		3rd	0.8	299.3	0.1	32.4	2.2	2.3	35.3
		4th	−43.0	299.5	0.1	32.7	3.2	3.7	117.6
	1.0	Before	–	651.4	0	42.0	0	3.0	0
		1st	0.2	651.6	0	41.6	−0.1	4.2	40.0
		2nd	−20.8	652.1	0.1	42.0	0	4.0	33.3
		3rd	Thermal runaway						

0.93 eV at 1,350 °C with increasing Tb_4O_7 amounts. The results for Φ_b in 1,300 and 1,350 °C are opposite of each other. On the whole, the Φ_b value of varistors sintered at 1,350 °C exhibited to be lower compared with those at 1,300 °C. This coincides with the variation of nonlinear coefficient in *E–J* characteristics. That is, the higher barrier height leads to good nonlinear properties in general. It is assumed that the lowering of Φ_b value gives rise to low nonlinearity, when compared with the nonlinear coefficient (α) between varistors sintered at 1,300 and 1,350 °C. The Φ_b is directly associated with the N_d and N_t. In other words, the Φ_b is estimated by the variation rate in the N_t and N_d. In general, the Φ_b is increased in relation to increasing N_t and decreasing N_d. If the variation rate of N_d is much larger than that of N_t, the Φ_b is much more strongly affected by the N_d than the N_t.

ZnO varistors begin to degrade because of gradually increasing leakage current with stress time. Eventually, they result in thermal runaway from stems' joule heating and the loss of varistor function. From this viewpoint, in addition to nonlinearity, electrical stability is a technologically very important characteristic of ZnO varistors.

Figure 6 shows the variation of leakage current of varistors during various accelerated aging stresses with different Tb_4O_7 amounts and sintering temperatures. Macroscopically, the sintered density and the leakage current affect the resistance against stress. That is, the higher the sintered density and the lower the leakage current, the higher the stability. As shown in $I_L - t^{1/2}$ curves, the stability exhibited to be more lowered with increasing Tb_4O_7 amount for varistors sintered at 1,300 °C. The varistors doped with 1.0, 0.5, 0.25 mol% exhibited thermal runaway within a short time at the 2nd, 3rd, and 4th stress, respectively. On the other hand, the varistors doped with only 1.0 mol% sintered at 1,350 °C exhibited thermal runaway within a short time at the 3rd. In the light of this result, it can be seen that the higher sintering temperature gives higher stability. The stability of varistors can be

estimated by the degradation rate coefficient (K_T), indicating the degree of aging. This exhibits the slope of leakage current for the stress time. The lower the K_T, the higher the stability, where the stability of the varistors doped with 0.25 and 0.5 mol% sintered at 1,350 °C needs to be compared in terms of K_T. The variations of K_T according to stress for the 0.25 and 0.5 mol% doped-Tb_4O_7 varistors sintered at 1,350 °C are shown in Fig. 7. The 0.25 mol% Tb_4O_7-doped varistors exhibited weakly positive creep phenomena that the K_T is -2.4 $\mu A \cdot h^{-1/2}$ during the 4th stress. However, the 0.5 mol% Tb_4O_7-doped varistors exhibited showed rather strongly negative creep phenomena that the K_T is -43.0 $\mu A \cdot h^{-1/2}$ during the 4th stress. In the light of the facts, it can be seen that the resistance against dc-accelerated aging stress is greatly affected by the Tb_4O_7 amount.

On the other hand, why do many samples exhibit thermal runaway though it has high sintered density and low leakage current like the varistors sintered at 1,300 °C? Presumably, this seems to be related to Tb-rich intergranular layer. The increase of Tb_4O_7 amount increases more Tb-rich intergranular layers. This decreases the cross-sectional area of conduction path at grain boundary and eventually leads to the concentration of current.

The variation rates of varistor voltage ($\%\Delta V_{1mA}$), variation rates of nonlinear coefficient ($\%\Delta\alpha$), and variation rates of leakage current ($\%\Delta I_L$) after dc-accelerated aging stress are summarized in Table 2. The 0.25 and 0.5 mol% Tb_4O_7-doped varistors exhibited low characteristic variation by presenting -1.5% and 0.1%, respectively, in $\%\Delta E_{1mA}$ and -2.2% and +3.2%, respectively, in $\%\Delta\alpha$. On the contrary, the $\%\Delta I_L$ relatively exhibited high variation by presenting +23.8% in 0.25 mol% Tb_4O_7 and +117.2% in 0.5 mol% Tb_4O_7. However, the leakage current density of 0.5 mol% Tb_4O_7-doped varistors was only 3.7 μA in after the 4th stress. Therefore, conclusively, it assumed that 0.5 mol% Tb_4O_7-doped varistors shows better withstanding resistance against dc-accelerated aging stress than 0.25 mol% Tb_4O_7-doped varistors.

Conclusions

The microstructure, electric field–current density (*E–J*), capacitance–voltage (*C–V*), and dc aging characteristics of the varistors were investigated for different Tb_4O_7 amounts and sintering temperatures. The density of ceramics increased with increasing Tb_4O_7 amount and sintering temperature. As the Tb_4O_7 amount increased, the nonlinear coefficient linearly increased, reaching maximum of 52.0 and 42.0 for varistors sintered at 1,300 and 1,350 °C, respectively. As the Tb_4O_7 amount increased, the varistor voltage linearly increased, reaching maximum of 845.1 V/mm and 651.4 V/mm for varistors sintered at 1,300 and 1,350 °C, respectively. The donor density was in the range of 0.7×10^{18}–$1.0 \times 10^{18}/cm^3$ and decreased with increasing Tb_4O_7 amount and sintering temperature. On the other hand, a good stability was obtained in the range of 0.25–0.5 mol% Tb_4O_7 when it was sintered at 1,350 °C. The varistor doped with 0.5 mol% Tb_4O_7 exhibited not only good stability, in which $\%\Delta V_{1\ mA} = -1.0\%$, $\%\Delta\alpha = -3.2\%$ for dc-accelerated aging stress of 0.95 $V_{1\ mA}$/150 °C/12 h, but also high nonlinear properties after stressing.

References

1. Levinson LM, Philipp HR (1986) Am Ceram Soc Bull 65:639
2. Gupta TK (1990) J Am Ceram Soc 73:1817
3. Lee YS, Tseng TY (1992) J Am Ceram Soc 75:1636
4. Alles AB, Burdick VL (1991) J Appl Phys 70:6883
5. Lee Y-S, Liao K-S, Tseng T-Y (1996) J Am Ceram Soc 79:2379
6. Nahm C-W (2001) Mater Lett 47:182
7. Nahm C-W (2002) J Mater Sci Lett 21:201
8. Nahm C-W (2003) Mater Lett 57:1317
9. Nahm C-W (2003) Solid State Commun 127:389
10. Nahm C-W, Park J-A, Kim M-J, Shin B-C (2003) J Mater Sci 39:307
11. Nahm C-W (2004) J Mater Sci 40:6307
12. Wurst JC, Nelson JA (1972) J Am Ceram Soc 55:109
13. Mukae M, Tsuda K, Nagasawa I (1979) J Appl Phys 50:4475
14. Hozer L (1994) Semiconductor ceramics: grain boundary effects. Ellis Horwood, p 22
15. Fan J, Freer R (1994) J Am Ceram Soc 77:2663